On the origin of repulsive forces of nematic liquid-crystalline films in the surface forces apparatus



1999 J. Phys.: Condens. Matter 11 8005

(http://iopscience.iop.org/0953-8984/11/41/305)

J. Phys.: Condens. Matter **11** (1999) 8005–8016. Printed in the UK PII: S0953-8984(99)05104-8

# On the origin of repulsive forces of nematic liquid-crystalline films in the surface forces apparatus

André M Sonnet† and Thomas Gruhn‡

† Dipartimento di Ingegneria Chimica, Università di Napoli Federico II, Piazzale Tecchio 80, I-80125 Naples, Italy
‡ Institut für Theoretische Physik, Sekretariat PN 7-1, Fachbereich Physik, Technische Universität Berlin, Hardenbergstraße 36, D-10623 Berlin, Germany

E-mail: sonnet@dragon.ian.pv.cnr.it and t.gruhn@physik.tu-berlin.de

Received 8 June 1999

**Abstract.** Starting from the Frank–Oseen free energy, the elastic forces of a thin nematic liquid-crystalline film between a cylinder and a planar substrate are calculated. The boundary conditions are assumed to be homeotropic. The repulsive forces obtained are found to be too small to be responsible for the elastic background frequently measured in surface forces apparatus experiments. Results from grand-canonical-ensemble Monte Carlo simulations which do not take into consideration a global deformation of the director field are sufficient for describing the experimental data. Repulsive forces appear to be a consequence of reorientations within intermediate strata between the fully developed molecular layers in the microscopic structure of the liquid-crystalline film.

## 1. Introduction

The material properties of a molecularly thin fluid film confined between solid substrates are substantially different from those of a bulk fluid. One instrument for measuring these properties with very high accuracy is the surface forces apparatus (SFA) [1]. In the SFA a fluid film is confined between two crossed cylinder substrates with equal macroscopic radii $R$ of the order of 1–2 cm. This set-up is immersed in a bulk reservoir of the same fluid as that constituting the film. Thus, at thermodynamic equilibrium, temperature $T$ and chemical potential $\mu$ are equal in the two subsystems (i.e., the film and bulk reservoir). The substrates are covered with mica, so the surfaces are perfectly smooth even on a microscopic level. An additional silver backing enables an interferometric measurement to be made of the substrate separation. By varying the normal force applied to the substrates, one can in principle measure the excess normal force per cylinder radius $F_z(h)/R$ as a function of the minimum distance $h$ between the substrates. If one goes to substrate separations of a few molecule diameters, most of the materials investigated, ranging from long-chain (e.g., hexadecane) or spheroidal (e.g., octamethylcyclotetrasiloxane (OMCTS)) [2] hydrocarbons to liquid crystals [3–5], show damped oscillatory behaviour of $F_z(h)/R$. With the help of the Derjaguin approximation [6], the normal force for curved substrates $F_z(h)$ can be related to the normal-stress component $T_{zz}(s_z)$ that a fluid film of thickness $s_z$ applies to confining plane-parallel substrates. In grand-canonical-ensemble Monte Carlo (GCEMC) simulations for confined simple fluid films between plane-parallel substrates, the formation of molecular strata parallel with the substrate plane is found, which leads to a

0953-8984/99/418005+12$30.00  

damped oscillating normal-stress curve $T_{zz}(s_z)$ (see [7] and references therein). Similar results are found by density functional theory approaches [8–10].

In SFA experiments with nematic liquid crystals, the oscillations of the normal force $F_z(h)$ are frequently superimposed upon by a repulsive background force [4, 5]. The origin of this force is not clear. Due to the long-range orientational order in nematic liquid crystals, it is in principle conceivable that this background force originates from the elastic distortions of the liquid crystal's orientation field in film regions where the assumption of local planarity of the substrates is no longer justified. If a nematic liquid crystal is confined by curved substrates that favour homeotropic alignment at the fluid–substrate interface, the mean orientation of molecules becomes spatially inhomogeneous. In a continuum description of nematics (cf. [14]) this is incorporated by means of an inhomogeneous macroscopic director field $\hat{\boldsymbol{n}}(\boldsymbol{r})$. Deviations from spatial homogeneity of the director field give rise to elastic forces. In [4], a rough estimate of the elastic forces has been given.

It is the aim of this paper to give a more precise account of this problem. In order to do so, the elastic contribution to the force on the crossed cylinders of an SFA is estimated by an analytical approach in which symmetry with respect to the mid-plane between the two cylinders is assumed. Treating one half of this scenario, the problem reduces to a cylinder in front of a plane, where on both the surface of the cylinder and the plane, homeotropic boundary conditions for the alignment are prescribed. In section 2, first the equilibrium director field for such a set-up is calculated, using the common one-constant approximation. The elastic free energy is then integrated for a liquid crystal in an SFA set-up and we arrive at the force by differentiating the expression obtained with respect to the film's thickness. In section 3 the results are discussed and related to a normal-force curve $F_z(h)$ obtained in GCEMC simulations for nematic liquid crystals.

## 2. The elastic force in the SFA

### *2.1. Calculation of the director field*

In the continuum description of liquid crystals a director field $\boldsymbol{n}$ indicating the local mean orientation of the molecules is adopted. The director $\boldsymbol{n}$ is a unit vector, and equilibrium configurations are obtained by minimizing the Frank–Oseen elastic free energy [11,12], whose density is given by

$$f_{FO} = \frac{1}{2}K_1(\boldsymbol{\nabla}\cdot\boldsymbol{n})^2 + \frac{1}{2}K_2(\boldsymbol{n}\cdot(\boldsymbol{\nabla}\times\boldsymbol{n}))^2 + \frac{1}{2}K_3(\boldsymbol{n}\times(\boldsymbol{\nabla}\times\boldsymbol{n}))^2 \qquad (1)$$

where $K_1$, $K_2$, and $K_3$ are the elastic constants for splay, twist, and bend deformations, respectively.

We want to calculate the director field of a liquid crystal between a plane and a cylinder parallel to that plane. A system of orthogonal coordinates $(t, u, v)$ is chosen in the following way. The axis of the cylinder points in the $t$-direction; $\boldsymbol{e}_u$ lies in the plane and $\boldsymbol{e}_v$ is perpendicular to the plane. The origin is located in the plane such that on the cylinder axis $u = 0$; see figure 1. For this geometry, one can assume the alignment to be homogeneous along the cylinder axis, so the dependence of $\boldsymbol{n}$ on $t$ can be omitted. It is furthermore assumed that the director is constrained to the $u$–$v$ plane. In this case, only splay and bend deformations are relevant. Since $K_1 \approx K_3 =: K$, one can apply the one-constant approximation, and $f_{FO}$ reduces to

$$f_{FO} = \frac{K}{2}(\nabla\boldsymbol{n})^2. \qquad (2)$$

Since $\boldsymbol{n}$ lies in the $u$–$v$ plane, it can be expressed as

$$\boldsymbol{n} = \sin\phi\,\boldsymbol{e}_u - \cos\phi\,\boldsymbol{e}_v \qquad (3)$$

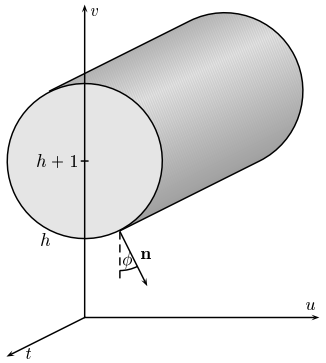


**Figure 1.** The system of coordinates for a cylinder parallel to a plane. All lengths are measured in units of the cylinder radius. The distance from the plane is $h$, the axis is located at $u = 0$, $v = h + 1$. The alignment in the $u$–$v$ plane is measured in terms of the angle $\phi$ that the director makes with $-\boldsymbol{e}_v$.

where $\phi$ denotes the angle between the director and the negative $v$-axis.

In this section all lengths will be expressed in units of the cylinder radius, so $R = 1$. If the distance between the cylinder and plane is called $h$, the cylinder axis is found at $(0, h + 1)$, and the boundary conditions take the form

$$\phi(u, v) \equiv_\pi \begin{cases} 0 & u = 0 \\ \arctan \dfrac{u}{v - (h + 1)} & u^2 + (v - (h + 1))^2 = 1. \end{cases} \tag{4}$$

The equality is required only modulo $\pi$ since, due to the nematic symmetry, alignments that differ by a multiple of $\pi$ are physically equivalent.

With the *ansatz* (3), the free-energy density (2) becomes

$$\frac{K}{2}(\nabla\phi)^2 \tag{5}$$

and the equilibrium director field is obtained by solving the corresponding Euler–Lagrange equation

$$\Delta\phi = 0. \tag{6}$$

We tackle this problem with the help of complex analysis. First, we recall that for a *conformal mapping* $g$ with

$$w = g(z) \tag{7}$$

where $w = u + \mathrm{i}v$ and $z = x + \mathrm{i}y$, both $\Delta u = 0$ and $\Delta v = 0$ hold. The image under $g$ of an $x =$ constant coordinate line makes an angle $\psi$ with the negative $v$-axis (cf. the present choice (3) for the director). This angle is given by

$$\psi = -\arctan \frac{\partial y}{\partial u} \Big/ \frac{\partial y}{\partial v} \tag{8}$$

and a straightforward calculation shows that $\Delta\psi = 0$. Therefore, a conformal mapping that maps the coordinate lines to the desired integral lines of the director field yields the solution to (6) and (4). For the present case, we find [13]

$$g_a = a \tan \frac{z}{2} \tag{9}$$

where $a$ is a parameter that depends on the cylinder's distance from the plane. The explicit relation between the $(u, v)$ and the $(x, y)$ coordinates is given by

$$\begin{aligned} u + \mathrm{i}v &= a\frac{\sin x + \mathrm{i}\sinh y}{\cos x + \cosh y} \\ x + \mathrm{i}y &= \arctan\frac{2au}{a^2 - u^2 - v^2} + \mathrm{i}\,\mathrm{arctanh}\frac{2av}{a^2 + u^2 + v^2}. \end{aligned} \tag{10}$$

With (8), this leads to

$$\psi = \arctan\frac{2uv}{a^2 + u^2 - v^2} \tag{11}$$

(cf. figure 2). It remains to express $a$ in terms of $h$. In order to do this, we note that the lines with $x =$ constant and $y =$ constant are circles in the $u$–$v$ plane with the equations

$$(u + a\cot x_c)^2 + v^2 = \frac{a^2}{\sin^2 x_c} \tag{12}$$

and

$$u^2 + (v - a\coth y_c)^2 = \frac{a^2}{\sinh^2 y_c} \tag{13}$$

respectively. According to the experimental set-up, $a$ has to be such that, for a fixed $y_0$, the circle with radius 1 has mid-point $(0, h + 1)$. From (13) we obtain

$$\begin{aligned} a\coth y_0 &= h + 1 \\ \frac{a^2}{\sinh^2 y_0} &= 1 \end{aligned} \tag{14}$$

which leads to

$$y_0 = \mathrm{arcsinh}\, a \tag{15}$$

and

$$a = \sqrt{2h + h^2}. \tag{16}$$

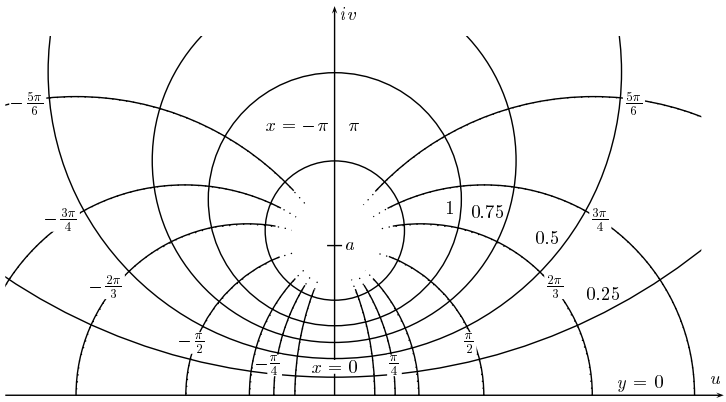


**Figure 2.** The image of the $(x, y)$ coordinate lines under the mapping $u + \mathrm{i}v = a\tan((x + \mathrm{i}y)/2)$. The $x =$ constant lines are the integral lines of the director field that satisfies the boundary conditions (4). The appropriate value of $a$ is given by (16).

With the results (11) and (16), the equilibrium director field of a liquid crystal between a plane and a cylinder parallel to it at a distance $h$ is determined by

$$\phi = \arctan \frac{2uv}{2h + h^2 + u^2 - v^2}. \tag{17}$$

### *2.2. Integration of the elastic free energy*

The elastic free energy of the liquid crystal is given by the integral over the density (5) with $\phi$ given by (17). Because of the symmetry with respect to the $v$-axis, it is sufficient to consider the region $u, v \geqslant 0$, where the transformation (10) is one to one. The total free energy is then expressed as

$$F = K \int_0^{x_0} \int_0^{y_0} \frac{\partial(u, v)}{\partial(x, y)} (\nabla\phi)^2 \, \mathrm{d}y \, \mathrm{d}x. \tag{18}$$

Here $y_0$ is given by (15), and $x_0$ will be specified later. The Jacobi determinant is determined by making use of the Cauchy–Riemann equations for $g$; we find

$$\frac{\partial(u, v)}{\partial(x, y)} = |g'(z)|^2 = \frac{a^2}{4} \left|\cos^{-2} \frac{z}{2}\right|^2 = \frac{a^2}{(\cosh y + \cos x)^2}. \tag{19}$$

Starting from (17) and employing (10), a straightforward calculation yields

$$(\nabla\phi)^2 = \frac{4(u^2 + v^2)}{(u^2 + v^2 + a^2)^2 - 4a^2v^2} = \frac{\cosh^2 y - \cos^2 x}{a^2}. \tag{20}$$

With this the free energy becomes

$$F = K \int_0^{x_0} \int_0^{y_0} \frac{\cosh y - \cos x}{\cosh y + \cos x} \, \mathrm{d}y \, \mathrm{d}x. \tag{21}$$

In the SFA, typical distances between the cylinders are smaller than $10^{-8}$ m, and the maximum thickness of the film is about $10^{-3}$ m. With a cylinder radius of $10^{-2}$ m, this yields $h < 10^{-6}$, and the liquid crystal is confined to a region stretching from an angle $-\alpha$ to $\alpha$, where $\alpha \approx \pi/8$; see figure 3. Hence it is safe to assume that both $a \ll 1$ and $a \ll \alpha$ hold. With $u_0 = \sin\alpha$ and $v_0 = h + 1 - \cos\alpha$, the integration limit $x_0$ is determined by (10):

$$\begin{aligned} x_0 &= \arctan \frac{a \sin\alpha}{(h+1)\cos\alpha - 1} \approx \arctan \frac{a \sin\alpha}{\cos\alpha - 1} \\ &= \arctan\left(-a \cot \frac{\alpha}{2}\right) = \pi - \arctan\left(a \cot \frac{\alpha}{2}\right) \approx \pi - a \cot \frac{\alpha}{2}. \end{aligned} \tag{22}$$

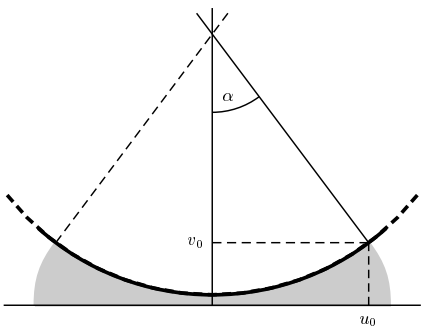


**Figure 3.** A cross section of the volume below the cylinder that is occupied by the liquid crystal. The angle $\alpha$ determines the limit of integration in the $x$-variable.

Note that this implies that even a small $\alpha$ corresponds to an $x_0$ close to $\pi$.

In calculating the elastic energy (21), we only take the leading terms in $a$, i.e., in particular we use $\operatorname{arcsinh} a \approx a$ and $\cosh y \approx 1$. This leads to

$$F/K \approx \int_0^{\pi - a\cot(\alpha/2)} \int_0^{a} \frac{1-\cos x}{1+\cos x}\,\mathrm{d}y\,\mathrm{d}x = a\int_0^{\pi - a\cot(\alpha/2)} \left(\frac{2}{1+\cos x} - 1\right)\mathrm{d}x$$
$$= 2a\cot\left(\frac{a}{2}\cot\frac{\alpha}{2}\right) - a\left(\pi - a\cot\frac{\alpha}{2}\right) = 4\tan\frac{\alpha}{2} - a\pi + \mathcal{O}(a^2). \tag{23}$$

In order to obtain the elastic contribution to the force on the cylinder, this expression must be differentiated with respect to $a$, while the volume of the liquid crystal is kept constant. Thus we first have to calculate the area of the intersection of the liquid crystal with the $u$–$v$ plane:

$$A = 2\int_0^{x_0}\int_0^{y_0} \frac{\partial(u,v)}{\partial(x,y)}\,\mathrm{d}y\,\mathrm{d}x = 2a^2\int_0^{x_0}\int_0^{y_0} (\cosh y + \cos x)^{-2}\,\mathrm{d}y\,\mathrm{d}x. \tag{24}$$

Using similar approximations to those for the energy, it is found that

$$A = \frac{8}{3}\tan^3\frac{\alpha}{2} + \mathcal{O}(a^2) \tag{25}$$

i.e., up to the first order in $a$ the area is constant. This can be understood by recalling that, due to (16), a contribution proportional to the separation $h$ is quadratic in $a$. Thus the requirement of a fixed volume is met by simply taking $\alpha$ to be constant.

The elastic force on the cylinder per unit length is then obtained by differentiating the free energy with respect to $h$:

$$-\frac{\partial F}{\partial h} = -\frac{\partial F}{\partial a}\frac{\partial a}{\partial h} \approx \pi K\frac{h+1}{\sqrt{2h+h^2}} \approx \frac{\pi K}{\sqrt{2h}}. \tag{26}$$

The total force on the SFA can be calculated by taking two times this expression for the two cylinders on either side of the plane, multiplied by the breadth of the sample in units of the radius. This result can be viewed at least as an upper bound for the elastic forces in the experiment. The net effect will be weaker because we have neglected possible finite anchoring energies and also because of the assumed symmetry with respect to the mid-plane.

In equation (26) the expression for the elastic force does not depend on the angle $\alpha$, where the only approximations used to obtain this result are $\alpha \gg a$ and $a \ll 1$. Thus one is not limited to the SFA but can also consider a cylinder that is completely embedded in an infinite liquid crystal. Then, of course, the free energy diverges, while the force still has the form (26). For very large distances apart, the force on the cylinder will converge to that on a line disclination. It is interesting to compare the two cases also for small $a$. The solution for the line disclination can be found in p 173ff of [14]. The director field is that given by (17), where the distance of the disclination from the plane is $a$. The force on the disclination is $2\pi K/a \approx 2\pi K/\sqrt{2h}$, which is twice the value found for the force on the cylinder. This is the effect of excluding the interior of the cylinder from the integration. Because the disclination gets arbitrarily close to the cylinder's boundary as $a \to 0$, one can interpret this as indicating that half of the relevant deformation takes place inside the cylinder.

## 3. Molecular reorientation

For liquid crystals composed of small molecules, the elastic constant is roughly $K = 10^{-11}$ N (cf. tables 3.1 and 3.2 in [14]). The breadth of the sample is about one and the distance apart of the two cylinders ranges from $2h = 10^{-7}$ to $2h = 10^{-5}$ in units of the cylinder radius. With $R = 1$ cm it follows from equation (26) that the elastic force exerted by the film on one of the

cylinders does not exceed $F_{el}/R \approx 2 \times 10^{-5}$ N m$^{-1}$. The magnitude of this force is larger than that of the rough estimate $F_{el}/R = 1.3 \times 10^{-7}$ N m$^{-1}$ given in [4].

In order to estimate the total normal force per radius that a confined nematic liquid crystal applies to the confining substrates, one has to add the forces due to the formation of strata within the film. These forces can be extracted from GCEMC simulations as described in the following.

### *3.1. GCEMC simulations of confined nematic films*

In GCEMC simulations, liquid-crystalline films between two plane-parallel substrates are investigated for different wall separations $s_z$ [15]. The film consists of ellipsoidal molecules which interact with each other via the modified Gay–Berne potential introduced in reference [16]. The simulations are performed for a thermodynamic state for which a corresponding bulk liquid crystal is nematic. Therefore the films are henceforth called 'nematic' though they exhibit more structure than a typical bulk nematic. The interaction between film molecules and wall atoms is chosen such that a homeotropic alignment of molecules is favoured [16]. The 'nematic' film is assumed to be confined in the $z$-direction by two planar substrates parallel with the $x$–$y$ plane. Surface deformations and thermal effects on the surface atoms are neglected. In the following, lengths are given in units of $\sigma_{ff}$, which is the small diameter of the liquid-crystal molecules, while energies are given in units of $\epsilon^s_{ff}$, which corresponds to the energy depth of the Gay–Berne potential for two parallel molecules lying side by side (see [17] for details). All other units can be expressed as combinations of the two.

In the grand canonical ensemble, infinitesimal, reversible transformations of thermodynamic states are governed by the grand potential $\Omega$. For a confined film, the exact differential of $\Omega$ is given by [18]

$$\mathrm{d}\Omega = -S\,\mathrm{d}T - N\,\mathrm{d}\mu + \gamma'\,\mathrm{d}A + T_{zz}A\,\mathrm{d}s_z \tag{27}$$

where $S$ denotes entropy, $N$ is the number of film molecules, $\gamma'$ is a film–wall interfacial tension, $A$ is the area of film–wall contact, and $T_{zz}$ is the average stress applied normally to $A$. By convention, $T_{zz} < 0$ if the $z$-component of the force on the substrate points outward.

From equation (27) one obtains for a film composed of linear molecules [17]

$$\begin{aligned} AT_{zz} &= \left(\frac{\partial\Omega}{\partial s_z}\right)_{T,\mu,A} = \left(\frac{\partial(-kT\ln\Xi)}{\partial s_z}\right)_{T,\mu,A} \\ &= -\frac{1}{\beta A\Xi}\sum_{N=0}^{\infty}\frac{1}{N!\Lambda^{5N}}\left(\frac{I}{m}\right)^N \exp(\beta\mu N)\left(\frac{\partial Z}{\partial s_z}\right)_{T,\mu,A} = \left\langle F_z^{[2]}\right\rangle = -\left\langle F_z^{[1]}\right\rangle \end{aligned} \tag{28}$$

where $F_z^{[k]}$ is the $z$-component of the total force exerted by (a particular configuration of ) the film on the upper ($k = 1$) and lower ($k = 2$) planar substrates, and angular brackets signify the grand-canonical-ensemble average. The last equation in (28) is a consequence of the principle of mechanical stability. If the separation between the substrates becomes sufficiently large, one has

$$\lim_{s_z\to\infty} T_{zz}(s_z) = -P_{\mathrm{bulk}}.$$

From the results of the GCEMC simulations for nematic films between planar substrates, one can estimate the solvation force applied by a nematic film on the curved substrates in the SFA. The whole SFA set-up is immersed in a liquid-crystal bulk reservoir at pressure $P_{\mathrm{bulk}}$. Due to the curved shape of the substrates, the normal stress $T_{zz}$ becomes a local quantity, which

varies with the vertical distance $s_z = s_z(x, y)$ between the substrate surfaces. By means of the Derjaguin approximation [6], the distance function $s_z$ for two crossed cylinders is to the first order equal to that of a sphere in front of a plane. Considering the latter geometry simplifies the calculation. To obtain a relation between $T_{zz}$ and the experimentally accessible solvation force $F(h)$, one can divide the film region between the sphere and plane into small prisms for which the substrate separation is fairly constant (see figure 4). Ignoring deformations of the director field considered in section 2, $F(h)$ can be expressed by integrating the excess normal pressure $f(s_z) := -T_{zz}(s_z) - P_{\text{bulk}}$ for the respective prisms of height $s_z$ [19]:

$$F(h) = -\int\int (T_{zz}(s_z(x, y)) + P_{\text{bulk}})\,\mathrm{d}x\,\mathrm{d}y = 2\pi \int_h^{h+R} (R + h - s_z) f(s_z)\,\mathrm{d}s_z \tag{29}$$

where the local separation $s_z$ is given by

$$s_z = h + R - \sqrt{R^2 - x^2 - y^2}$$

(see figure 1). Since $f(s_z)$ differs significantly from zero only for $s_z \ll R$, the upper integration limit in equation (29) may be taken to infinity to give

$$\frac{F(h)}{2\pi R} = \int_h^{\infty} f(s_z)\,\mathrm{d}s_z. \tag{30}$$

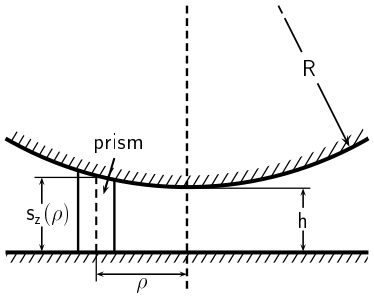


**Figure 4.** A side view of the film confined between a sphere of macroscopic radius $R$ and a planar substrate surface. The solvation force can be obtained by integrating over the local excess pressure $f(s_z)$ calculated in GCEMC simulations of the respective prism region.

The plots in figure 5 show that the excess pressure is a damped oscillatory function of the wall separation. Over the range $4.0 \leqslant s_z \leqslant 20.0$, $f(s_z)$ exhibits five maxima separated by a distance $\Delta s_z \simeq 3.2$, which is slightly smaller than the large diameter of a film molecule ($\approx$3.5).

The curve of $f(s_z)$ also exhibits shoulders at characteristic values of $s_z$ separated by the same distance $\Delta s_z \approx 3.2$ as the maxima. Portions of $f(s_z)$ between neighbouring minima (i.e., $s_z < 6.80$, $6.80 \leqslant s_z \leqslant 10.00$, $10.00 \leqslant s_z \leqslant 13.20$, and $13.20 \leqslant s_z \leqslant 16.40$) are remarkably similar. In order to correlate the microscopic structure of the confined film with features of $f(s_z)$, it is convenient to label these portions as *decrease*, *increase*, and *shoulder* zones [15]. The shoulder zones are related to reorientations of film molecules. This is demonstrated in the 'snapshots' in figure 6 for the transition from two to three strata in the liquid-crystalline film.

For $s_z = 7.5$, the film is in a decrease zone and consists of two homeotropic layers (see figure 6(a)). In the adjacent increase zone, substrate separations are too large to accommodate two homeotropic layers conveniently, but too small for three fully developed homeotropic layers (see figure 6(b)). In fact, two outer layers are found with homeotropically oriented molecules contacting one of the substrates, while in the middle of the film there is enough space

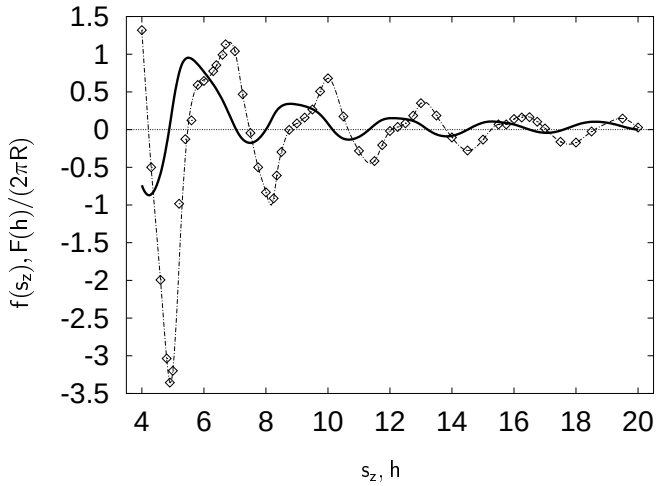


**Figure 5.** The excess pressure $f(s_z)$ ($\diamond$, dashed line) and the solvation force per radius $F(h)/R$ (full line) as functions of $s_z$ and $h$, respectively, for a 'nematic' film between homeotropically orienting substrates. Lengths are given in units of $\sigma^s_{ff}$, $f(s_z)$ and $F(h)/R$ are given in units of $\epsilon^s_{ff}/(\sigma^s_{ff})^3$ and $\epsilon^s_{ff}/(\sigma^s_{ff})^2$, respectively (see the text).

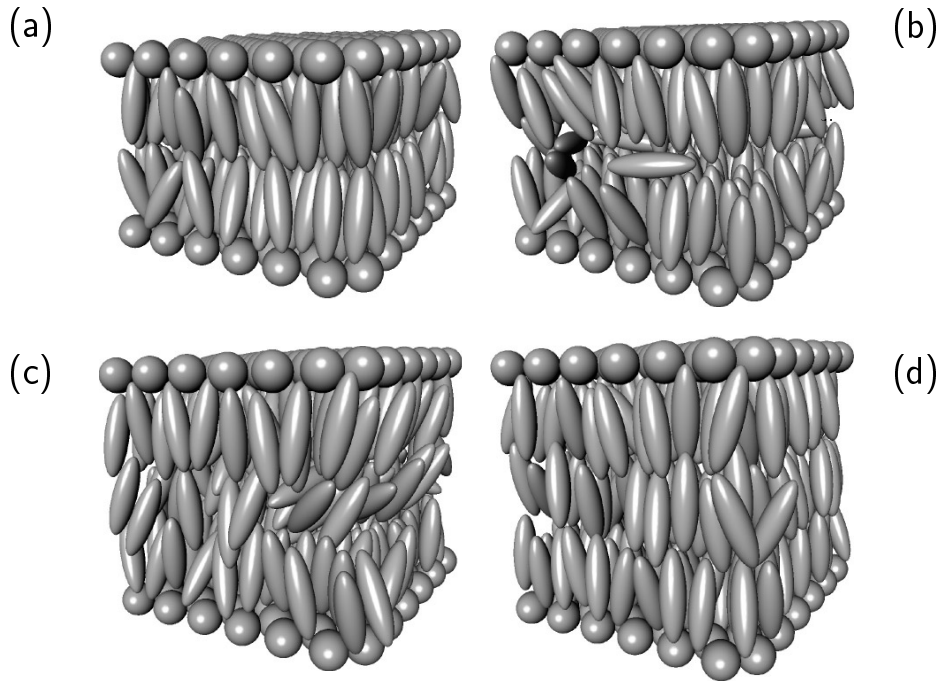


**Figure 6.** 'Snapshots' of configurations of 'nematic' Gay–Berne films with walls at various separations. (a) $s_z = 7.5$; (b) $s_z = 8.5$; (c) $s_z = 9.75$; (d) $s_z = 10.5$.

for a few molecules to form a weak middle stratum. In contrast to the case for the two contact strata, molecules in the middle stratum are oriented parallel with respect to the wall plane. As

the wall separation increases beyond $s_z \simeq 8.8$ (the shoulder zone), the orientation of the contact strata remains unaltered, while molecules in the middle of the film change their orientation from planar to homeotropic (see figure 6(c)). If $s_z$ increases further, a homeotropically oriented three-layer structure eventually forms (see figure 6(d)). In a similar fashion variations in the film's microscopic structure can be correlated with variations of $T_{zz}$ in decrease, increase, and shoulder zones for other values of $s_z$ [15].

### *3.2. Forces exerted on curved substrates*

The simulation results for $f(s_z)$ may now be used to calculate the solvation force $F(h)/R$ applied by the film on the substrates in the SFA. The curve of $F(h)/R$ in figure 5 is obtained by numerically solving equation (30) (i.e., by numerically integrating $f(s_z)$). The structure of $F(h)/R$ between two neighbouring minima is distinctly similar. Nevertheless, $F(h)/R$ is not as regular as a corresponding curve for a 'simple' fluid (see reference [19]) and is, furthermore, not simply a shifted version of $f(s_z)$. The curve of $F(h)/R$ is free of any shoulders. The height and width of its maxima exceed the depth of its minima considerably. In other words, $F(h)/R$ oscillates around a repulsive background force. This repulsive background is not related to the elastic force $F_{el}$ given in equation (26), which has not been considered for this curve. Taking $\epsilon^s_{ff} = 1.2 \times 10^{-21}$ J and $\sigma^s_{ff} = 0.5$ nm, as used in [20] to fit the Gay–Berne potential to properties of 8CB, one finds that $F(h)/R$ is given in units of $\epsilon^s_{ff}/(\sigma^s_{ff})^2 \approx 5$ mN m$^{-1}$. With this value, the amplitude of the oscillations and the repulsive background of $F(h)/R$ in figure 5 are in good agreement with experimental data (see figure 4(a) in reference [5]), as far as 'nematic' films of 8CB between homeotropically anchoring walls are concerned. The background forces measured in these SFA experiments range from $F/R = 10^{-4}$ N m$^{-1}$ to $5 \times 10^{-2}$ N m$^{-1}$. The amplitudes of the oscillatory short-range forces are of the same order of magnitude. One can conclude that the force contribution due to director field deformations, being smaller than $F_{el}/R \leqslant 2 \times 10^{-5}$ N m$^{-1}$, is not large enough to be responsible for the measured repulsive background forces. In fact, it can be completely neglected in comparison with the amplitude of $F(h)/R$ in figure 5, which already describes very well the experimentally measured normal-force curve.

Since $F(h)/R$ is proportional to the integral of $f(s_z)$, the repulsive background of $F(h)/R$ is related to the fact that regions with positive values for $f(s_z)$ are predominant. This in turn is related to the existence of the shoulder regions in $f(s_z)$ and is therefore finally a consequence of the reorientation effects in intermediate strata. One may thus conclude that repulsive forces observed in SFA measurements of thin nematic films do not stem from a global deformation of the director field, but from deviations from the global orientation in intermediate strata, which otherwise would not fit between the fully developed smectic-A-like layers of the film.

## 4. Conclusions

One conceivable source of the longer-ranging repulsive background force that is frequently observed in SFA experiments with nematic liquid-crystalline films is the long-range orientational order in nematics. In this article the elastic force of a nematic film between a cylinder and a planar substrate was investigated in the limit of small separations. For this purpose, the orientational order of the liquid-crystalline film was described by a continuum director field $\boldsymbol{n}(\boldsymbol{r})$, whose deformations lead to an increase of the Frank–Oseen free energy. The equilibrium director field for the given boundary conditions (homeotropic orientation at the cylinder and plane substrate) was found by minimizing this energy. The elastic force was then obtained by differentiating the free energy with respect to the minimum distance between the cylinders.

In this way, an upper bound was found for the elastic force that a liquid crystal exerts on a surface forces apparatus composed of two orthogonal cylinders: the elastic force turned out not to exceed $F_{el}/R \approx 2 \times 10^{-5}$ N m$^{-1}$. This value is larger than that of the rough estimate $F_{el} = 1.3 \times 10^{-7}$ N m$^{-1}$ given in [4]. However, it is still too small to explain the experimentally observed repulsive background in the range of $F/R = 10^{-4}$ N m$^{-1}$ to $5 \times 10^{-2}$ N m$^{-1}$ [4, 5], around which the normal force oscillates.

More clues are found by considering short-range spatial and orientational order in regions where the film thickness is of the order of a few molecule lengths. The microscopic order in these film regions can be obtained from GCEMC simulations in which the film is considered to be confined between two plane-parallel substrates. The GCEMC simulations allow one to calculate the excess pressure $f(\cdot)$. With the help of the Derjaguin approximation one can obtain the normal force per substrate curvature radius $F(h)/R$ by numerically integrating the simulation data for the excess pressure $f(s_z)$. The normal-force curve $F(h)/R$ obtained does not oscillate symmetrically around the zero axis, but appears to oscillate around a repulsive background force just like the curves observed in the experiments. The amplitude of the oscillation and the background force are comparable to the experimental data. In the GCEMC simulations, long-range director deformations are not included. It can be concluded that, instead of elastic forces, the microscopic structure of the nematic film is responsible for the repulsive background observed in solvation force curves for liquid-crystalline films. Since no repulsive background forces are found for simple fluids, they must be ascribed to the orientation effects in the molecularly small film regions. The reorientation of film molecules is reflected in shoulder regions of the excess pressure $f(\cdot)$, which in turn result in repulsive force contributions to $F(h)/R$, which are large enough to explain the background force measured in SFA experiments.

## Acknowledgments

We thank E G Virga, M Schoen, and K-E Hellwig for helpful discussions and acknowledge support from the Deutsche Forschungsgemeinschaft via the SFB 448 'Mesoskopisch strukturierte Verbundsysteme'. Computations were carried out at the Konrad-Zuse-Rechenzentrum (Berlin), which we acknowledge for a generous allocation of computer time.

## References

[1] Israelachvili J N 1992 *Intermolecular and Surface Forces* 2nd edn (London: Academic)
[2] Gee M L, McGuiggan P M, Israelachvili J N and Homola A M 1990 *J. Chem. Phys.* **93** 1895
[3] Koltover I, Idziak S H J, Safinya C R, Steinberg S, Israelachvili J N and Liang K S 1995 *MRS Symp. Proc. No 366* vol 18, ed J M Drake (Pittsburgh, PA: Materials Research Society) p 101
[4] Horn R G, Israelachvili J N and Perez E 1981 *J. Physique* **42** 39
[5] Ruths M, Steinberg S and Israelachvili J N 1996 *Langmuir* **12** 6637
[6] Derjaguin B 1934 *Kolloid Z.* **69** 155
[7] Schoen M 1993 *Computer Simulation of Condensed Phases in Complex Geometries* (Heidelberg: Springer)
[8] Tarazona P and Vicente L 1985 *Mol. Phys.* **56** 557
[9] Evans R, Henderson J R, Hoyle D C, Parry A O and Sabeur Z A 1993 *Mol. Phys.* **80** 755
[10] Götzelmann B and Dietrich S 1997 *Phys. Rev.* E **55** 2993
[11] Oseen C W 1933 *Trans. Faraday Soc.* **29** 883
[12] Frank F C 1958 *Discuss. Faraday Soc.* **25** 19
[13] Flügge S (ed) 1958 *Elektrische Felder und Wellen (Handbuch der Physik vol 16)* (Berlin: Springer)
[14] de Gennes P G and Prost J 1993 *The Physics of Liquid Crystals* 2nd edn (Oxford: Clarendon)
[15] Gruhn T 1999 *Substrate-Induced Order in Confined Molecularly Thin Liquid-Crystalline Films* (Berlin Wissenschaft und Technik)

[16] Gruhn T and Schoen M 1998 *J. Chem. Phys.* **108** 9124
[17] Gruhn T and Schoen M 1997 *Phys. Rev.* E **55** 2861
[18] Diestler D J, Schoen M, Curry J E and Cushman J H 1994 *J. Chem. Phys.* **100** 9140
[19] Schoen M, Gruhn T and Diestler D J 1998 *J. Chem. Phys.* **109** 301
[20] Palermo V, Biscarini F and Zannoni C 1998 *Phys. Rev.* E **57** R2519